

A Near-Infrared Fluorescent Probe for Detection of Nitroxyl in Living Cells



LIU Ping¹, HAN Xiao-Yue^{1,2}, YU Fa-Biao^{1,*}, CHEN Ling-Xin^{1,*}

¹ Key Laboratory of Coastal Environmental Processes and Ecological Remediation, The Research Centre for Coastal Environmental Engineering and Technology, Yantai Institute of Coastal Zone Research, Chinese Academy of Sciences, Yantai 264003, China

² University of Chinese Academy of Sciences, Beijing 100049, China

Abstract: Nitroxyl (HNO), the one-electron reduced and protonated congener of nitric oxide (NO), has been demonstrated with excellent bio-pharmacological effects in cardiovascular disorder treatment, which is distinctive from that of NO. Despite its high reactivity, the accurate detection of HNO is a challenging issue. To resolve this problem, in this work, a near-infrared (NIR) metal-free fluorescent probe, ER-JN, was designed and synthesized for the detection of intracellular HNO concentration in simulated physiological conditions and living cells. The probe was consisted of two moieties, the BF₂-chelated tetraarylazadipyromethane fluorophore (aza-BODIPY) and the HNO recognition unit, diphenylphosphinobenzoyl group. The probe was purified by silica column chromatography eluting with CH₂Cl₂ to obtain the green solid product with a yield of 28%. The as-prepared probe exhibited high sensitivity, good selectivity and low cytotoxicity, and was applied to fluorescent bio-imaging of HNO in simulated physiological conditions. When used in detection of HNO, quantum yield of the probe increased from 0.01 to 0.35. The linear range was 0–50 μM, with the detection limit of 0.03 μM (*S/N* = 3). With confocal laser scanning microscope imaging analysis, the probe could be used to detect HNO concentration in living cells. Furthermore, the results of flow cytometry confirmed that the probe could be employed for the qualitative and quantitative detection of intracellular HNO level. In this work, we found that probe ER-JN could not only detect HNO in aqueous solution and in living cells, but also target endoplasmic reticulum. We anticipate that ER-JN will provide experimental bases in studying physiological and pathological functions of HNO in cells, *in vitro* and *in vivo*.

Key Words: Fluorescent probe; Nitroxyl; Cell analysis; Near-infrared bioimaging

1 Introduction

Nitroxyl (HNO) is the one-electron reduced and protonated form of nitric oxide (NO), and displays distinct biological and pharmacological activities compared with NO. Due to its potential pharmacological activities, it has caused wide attention in recent years. HNO displays unique biological effects in the treatment of cardiovascular disorders such as angina and heart failure^[1]. Angeli's salt (AS) (a HNO donor) is a potent vasodilator both *in vitro* and *in vivo*, and can elicit vasorelaxation in isolated large conduit, small resistance arteries and intact coronary arteries^[2,3]. Moreover, HNO elicits

distinct actions on myocardial contractile function that are not common to NO. Its cardiac effects are mediated by cardiac sarcoplasmic ryanodine receptors, which can effectively avoid the issue of nitroglycerin tolerance^[4], and may provide a potential treatment for cardiovascular diseases. Despite more and more evidences showing the pharmacological importance of HNO, the understanding of endogenous HNO action mechanism is hampered by the lack of effective detection methods because HNO is unstable, and promptly dimerizes and dehydrates to nitrous oxide (N₂O)^[1,2,5].

Many techniques are available for detecting HNO, including electrochemistry, electron paramagnetic resonance

Received 28 May 2015; accepted 21 August 2015

* Corresponding author. Email: fbyu@yic.ac.cn; lxchen@yic.ac.cn

This work was supported by the Beijing Natural Science Foundation of China (Nos. 21405172, 21575159, 21275158), and the Program of Youth Innovation Promotion Association, Chinese Academy of Sciences (No. 2015170).

Copyright © 2015, Changchun Institute of Applied Chemistry, Chinese Academy of Sciences. Published by Elsevier Limited. All rights reserved.

DOI: 10.1016/S1872-2040(15)60883-0

(EPR), colorimetry and chemiluminescence method, etc^[6,7]. Compared with these techniques, fluorescent probe based methods have the advantages of high resolution, high sensitivity, and noninvasive damage to biological specimens^[8,9]. Nevertheless, few fluorescent probes for HNO detection were reported, and were mostly based on the reduction of Cu²⁺^[10–12]. These fluorescent probes were susceptible to interferences from cellular reductants such as glutathione (GSH) and ascorbate. Moreover, the emission wavelengths of these reported probes were mainly located in UV-visible region. Because many organisms emit fluorescence under UV-visible light, the detection of biological samples using these probes might be interfered severely by the background autofluorescence. While the excitation/emission wavelengths of near-infrared (NIR) probes are located in 650–900 nm, which can minimize photo damage and avoid noise from background autofluorescence^[13,14]. Our group was committed to the development of probes for detecting RNS, RSS and ROS^[13–19]. Recently, we reported two fluorescent probes (Lyso-JN and Cyto-JN) for detecting HNO^[20,21], which were used to test the change of cellular HNO level and applied to the fluorescent bio-imaging of HNO in mice. In this work, a near-infrared (NIR) metal-free fluorescent probe, ER-JN, was synthesized for the detection of intracellular HNO level in simulated physiological conditions and living cells. It was found that probe ER-JN could be used to detect HNO concentration in living cells with high sensitivity and low cytotoxicity.

2 Experimental

2.1 Instruments and reagents

All pH measurements were performed with a pH-3C digital pH meter (Shanghai Lei Ci Device Works, Shanghai, China). Fluorescence spectra were measured on FluoroMax-4 Spectrofluorometer with a Xenon lamp and 1.0-cm quartz cells. Absorption spectra were obtained on NANO Drop 2000c UV-visible spectrophotometer (Thermo Fisher

Scientific, USA). Fluorescence imaging of cells was performed on an Olympus Laser Scanning Confocal Microscope (FV1000, Olympus, Japan) at 60 × magnifications. Intracellular fluorescence detection was carried out on a flow cytometry (Aria, BD, USA) with excitation at 633 nm and emission in the range of 750–810 nm. Mouse leukaemic monocyte macrophage cell line (RAW264.7) was obtained from the cell bank of the Shanghai Institute of Biochemistry and Cell Biology (Shanghai, China). Ultrapure water was used throughout. DMEM and trypsin were purchased from Gibco (Grand Island, USA). 3-(4,5-Dimethylthiazol-2-yl)-2,5-diphenyltetrazolium bromide (MTT) was purchased from Sigma-Aldrich.

2.2 Synthesis of probe ER-JN

As shown in Fig.1, under argon atmosphere, a solution of Aza-BODIPY (52.9 mg, 0.1 mmol) in CH₂Cl₂ (50 mL) was treated with 2-(diphenylphosphino) benzoic acid (61.2 mg, 0.2 mmol), 4-dimethylaminopyridine (DMAP, 24.4 mg, 0.2 mmol) and 1-(3-(dimethylamino)propyl)-3-ethylcarbodiimide hydrochloride (EDC, 19.2 mg, 0.1 mmol). The mixture was stirred at room temperature for 24 h. The course of the reaction was monitored by thin layer chromatography (TLC). Then coarse product was neutralized with saturated NaBr solution, and partitioned with CH₂Cl₂ and H₂O. Then the solvent was evaporated under reduced pressure, and the obtained residue was purified by column chromatography. ER-JN was obtained as a green solid with a yield of 28%. ¹H NMR (500 MHz, DMSO-*d*₆) δ (ppm): 8.31–8.01 (m, 1H), 7.53–7.40 (m, 6H), 7.25–7.23 (m, 23H), 7.16 (m, 2H), 6.98–6.94 (m, 2H), 4.05 (m, 2H), 1.98 (m, 2H), 1.26–0.98 (m, 37H). ¹³C NMR (125 MHz, DMSO-*d*₆) δ (ppm): 165.02, 162.82, 157.01, 152.12, 137.63, 137.54, 134.31, 134.14, 133.97, 133.63, 131.84, 131.66, 131.00, 129.96, 129.77, 129.63, 129.52, 125.39, 129.31, 129.26, 129.21, 129.16, 122.40, 121.27, 116.72, 60.22, 30.01, 21.02, 14.55. ³¹P NMR (200 MHz, CDCl₃) δ (ppm): –4.05. LC-MS (ESI): C₇₁H₇₅BF₂N₃O₃P calcd. 1097. 56, found 1097. 57.

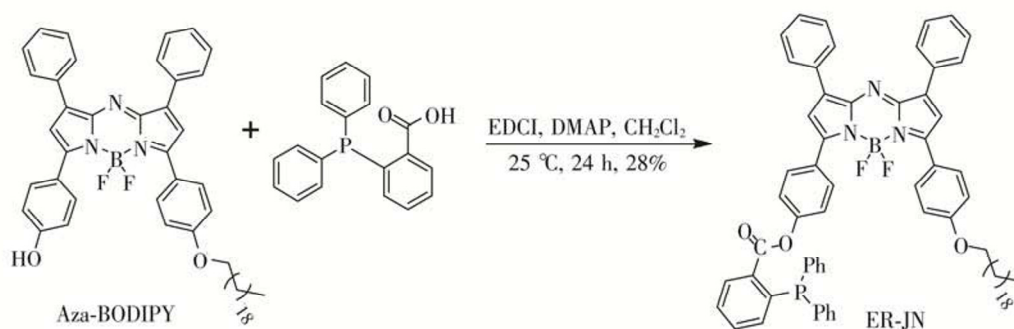


Fig.1 Synthetic route for probe ER-JN

2.3 Spectral analysis of probe ER-JN

Tween 80 (10%, 0.4 mL) was added to a 10.0 mL color comparison tube and diluted to 10.0 mL with HEPES buffer (10 mM, pH 7.4), and then different concentrations of AS was added. Finally, probe ER-JN was added. The mixture was equilibrated for 20 min, and then the absorption spectra and fluorescence spectra were measured.

2.4 Cell culture

RAW264.7 cells were grown in Dulbecco's modified Eagle's medium (DMEM) supplemented with 10% fetal bovine serum (FBS) in an atmosphere of 5% CO₂ and 95% air at 37 °C. After the cells reached confluence, the cells were washed with PBS and detached with 0.25% trypsin solution.

2.5 Cytotoxicity assays

RAW264.7 cells were cultured in DMEM supplemented with 10% FBS in an atmosphere of 5% CO₂ and 95% air at 37 °C. The cells were inoculated into 96-well microplates (8000 per well) and incubated for 24 h, and then treated with 0.1–100 μmol of probe at 37 °C for 24 h. After that, MTT solution (5.0 mg mL⁻¹, 20 μL) was added to each well and incubated for 4 h. After the removal of MTT solution, DMSO (150 μL/well) was added to dissolve formazan crystals. The microplate was shaken for 10 min and the absorbance at 490 nm of each well was measured using a microplate reader (TECAN infinite M200pro).

2.6 Confocal imaging

RAW 264.7 cells were inoculated in cell culture petri dishes with 1 mL DMEM medium. Hoechst 33342, DiOC₆ (3) (3,3'-Dihexyloxycarbocyanine iodide, 0.1 μM), probe ER-JN (DMEM, 0.1 μM) and HNO (200 μM) were added sequentially and incubated for certain time periods, respectively. Prior to imaging, the cell medium was removed, and then cells were washed with DMEM thrice to remove excessive probe. Fluorescence imaging of cells were

performed on an Olympus Laser Scanning Confocal Microscope (FV1000, Olympus) at 60 × magnification.

2.7 Flow cytometry analysis

The cells were inoculated in 6-well plate at 3.0×10^5 cells per well and incubated in an atmosphere of 5% CO₂ and 95% air at 37 °C for 24–48 h. The cells were incubated with ER-JN (5 μM) for 15 min, and then treated with 200 μM AS for 10 and 20 min, respectively. After harvest, the cells were washed with DMEM twice and suspended in PBS and then analyzed by flow cytometry

3 Results and discussion

3.1 Design of ER-JN

In this work, a NIR fluorescent probe ER-JN was designed and synthesized for detection of HNO. The probe could target to endoplasmic reticulum (ER). As shown in Fig.2, ER-JN was composed of three moieties: the Aza-BODIPY fluorophore, the HNO recognition unit and the endoplasmic reticulum locating alkyl chain. The excitation/emission wavelengths of Aza-BODIPY fluorophore were in NIR region. Triphenylphosphonium as the recognition unit could react with HNO, forming nitrogen-ylide intermediates, which might nucleophilically attack on the intramolecular suitably located ester to form an amide, resulting in the release of Aza-BODIPY and recovery of its fluorescence^[20,21]. Liposoluble long-chain alkyl is a typical endoplasmic reticulum locator. The experimental results proved that ER-JN could offer good performances in detecting HNO concentration in endoplasmic reticulum of living cells.

3.2 Spectroscopic properties of ER-JN

We investigated the spectroscopic properties of probe ER-JN under simulated physiological conditions (10 mM HEPES buffer solution, pH 7.4, 0.5% Tween 80). As shown in Fig. 3a, probe ER-JN (5 μM) exhibited an absorption maximum at 675 nm, $\epsilon = 5.2 \times 10^4 \text{ M} \cdot \text{cm}^{-1}$. Upon the addition

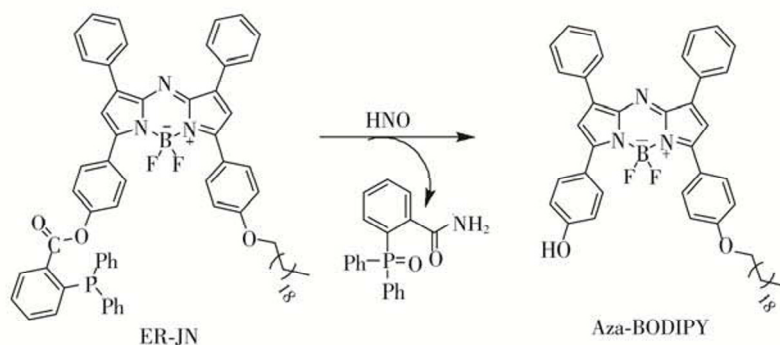


Fig.2 Proposed reaction mechanism for HNO detection

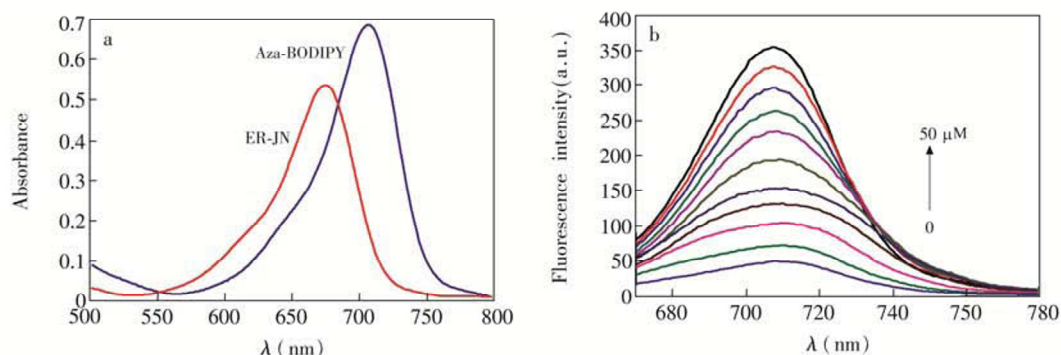


Fig.3 a. UV-vis absorption spectra of probe ER-JN (10 μM) before and after the addition of 50 μM HNO; b. Fluorescence spectra of ER-JN (10 μM) upon the addition of HNO (0–50 μM) for 20 min

of 50 μM AS, the absorption peak at 675 nm disappeared whereas a new absorption peak centered at 707 nm, $\epsilon = 6.9 \times 10^4 \text{ M} \cdot \text{cm}^{-1}$, indicating that the reaction between probe ER-JN and AS induced the break of ester bond and release of aza-BODIPY fluorophore. To evaluate the feasibility of ER-JN in the detection of HNO concentration under simulated physiological conditions, 690 nm was selected as the excitation wavelength. Fluorescence titration of ER-JN in the presence of AS at the HNO concentration range of 0–50 μM in buffer solution was then performed. The corresponding fluorescence emission profiles, with a maximum emission at 710 nm, increased with the HNO concentration, and the quantum yields of ER-JN increased from 0.01 to 0.35. Moreover, there was a good linear relationship between fluorescent response of ER-JN and HNO concentration ranging from 0 to 50 μM (Fig.4), and the calibration curve was $F_{710 \text{ nm}} = 6.3C_{\text{HNO}} (\mu\text{M}) + 39.7$ ($r = 0.9981$). The detection limit ($3\sigma/k$) was calculated to be 0.03 μM , indicating that ER-JN was highly sensitive to HNO. The result demonstrated that excitation and emission wavelength of ER-JN were both in the NIR region, and ER-JN would have good potential for application in cells and *in vivo*.

3.3 Selectivity of ER-JN

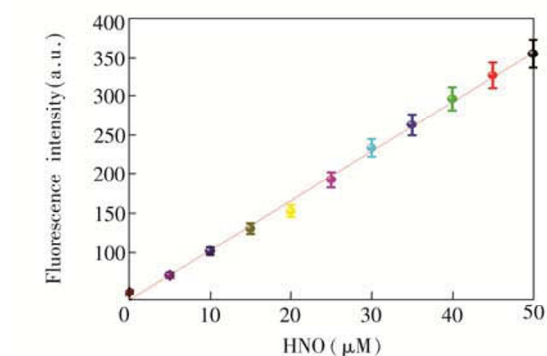
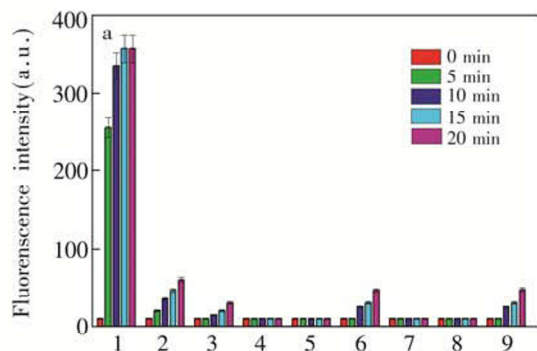


Fig.4 Linear relationship between the fluorescent intensity at 710 nm and AS concentration (0–50 μM) in buffer solution

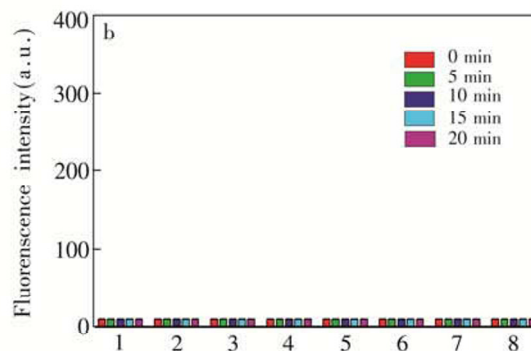


Fig.5 Fluorescence responses of 10 μM ER-JN to testing species in HEPES buffer solution

(a) 1, 50 μM HNO; 2, 20 μM GSNO; 3, 200 μM ONOO $^-$; 4, 50 μM NOC-5; 5, 500 μM NO $_2^-$; 6, 200 μM H $_2$ O $_2$; 7, 100 μM O $_2^-$; 8, 20 μM MeLOOH; 9, 200 μM ClO $_2^-$.
(b) 1, 50 μM Cys; 2, 100 μM GSH; 3, 500 μM NaHS; 4, 200 μM Vc; 5, 200 μM VE; 6, 100 μM Citrate; 7, 200 μM tyrosine (Tyr); 8, 50 μM HA

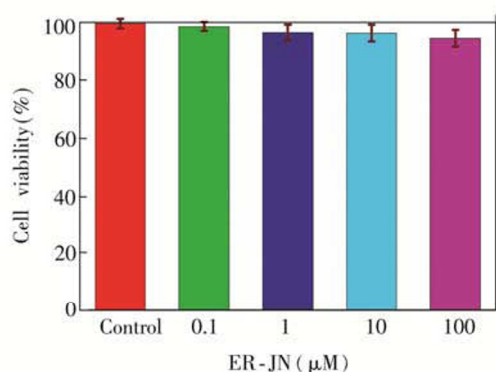


Fig.6 Cell viabilities of RAW264.7 cells after treated with 0.1–100 μM of ER-JN for 24 h. Data were expressed as the means \pm SD of data obtained from triplicate experiment

GSNO could form amide in a fashion similar to HNO. As shown in Fig.5, GSNO could elicit response and cause the comparatively limited fluorescence change in 20 min. However, the change of fluorescence caused by GSNO was comparatively smaller than that of HNO. The above experiments results indicated that ER-JN had better selectivity to HNO over GSNO. At the same time, NO_2^- , another decomposition product of AS, showed no obvious influence on ER-JN fluorescence. Therefore, in competition experiments, ER-JN could recognize HNO without disturbance of other biologically relevant species, further proving that the probe ER-JN possessed excellent selectivity towards HNO.

3.4 Cytotoxic effect of ER-JN

Low cytotoxicity is a key criterion for the physiological application of fluorescent probe in cells. The cytotoxicity of ER-JN was evaluated by MTT assay using RAW 264.7 cells. As illustrated in Fig.6, the cell viabilities were over 90% after incubation with 0.1–100 μM ER-JN for 24 h. The results demonstrated that the probe ER-JN had good biocompatibility, and could be used in the detection of HNO in cells.

3.5 Bioimaging of HNO in cells

On the basis of the high sensitivity and selectivity features of ER-JN for the detection of HNO in solution, its applicability in imaging HNO in living cells was investigated utilizing laser scanning confocal microscopy. After incubated with 1 μM ER-JN for 15 min, RAW 264.7 cells displayed faint fluorescence (Fig.7a). Next, 200 μM AS was added to the system and left for 10 min, and a strong intracellular fluorescence was observed (Fig.7d). With the passage of time, the cells were emitted stronger fluorescence (Fig.7g). The results suggested that ER-JN was suitable for test the change of cellular HNO concentration. We introduced an endoplasmic reticulum targeted dye DiOC₆ (3) (3,3'-dihexyloxycarbocyanine iodide) and a nucleus fluorescence marker Hoechst 33342 to discern the cellular location of ER-JN in RAW264.7 cells. As shown in Fig.7 (c, f and i), the fluorescence of ER-JN exhibited a consistent overlap with DiOC₆ (3), while showed hardly any overlap with the nucleus dye Hoechst 33342. The results verified that ER-JN, with subcellular localization in endoplasmic reticulum, could be used for fluorescence detection of HNO in living cells.

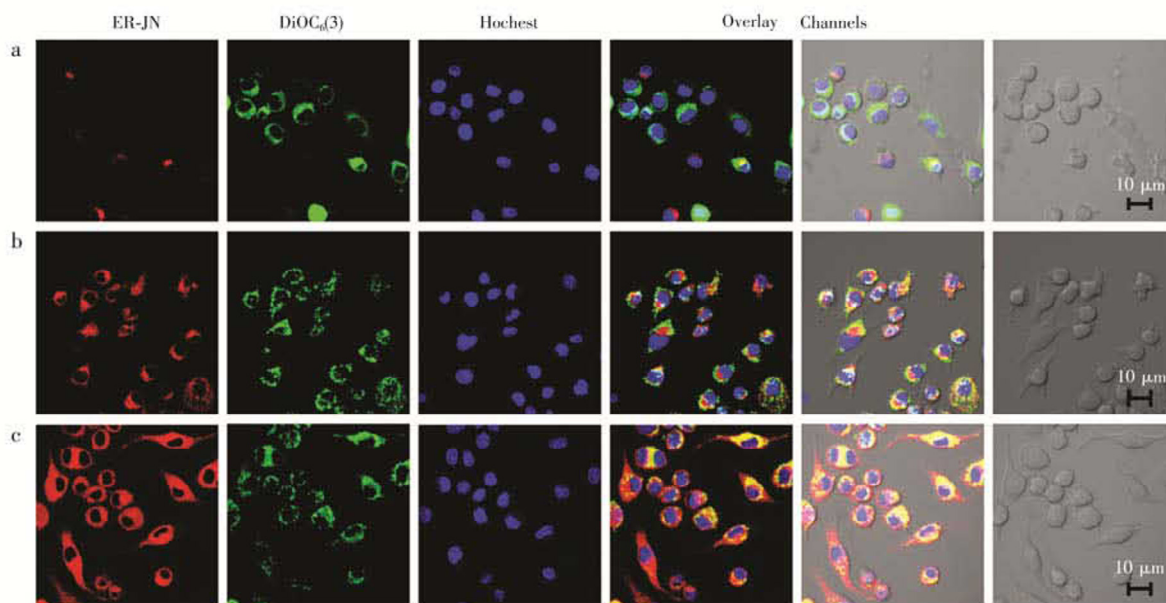


Fig.7 Confocal fluorescence images of HNO in RAW 264.7 cells treated with ER-JN

(a) Cells loaded with 1 μM probe for 15 min. (b) and (c) Cells treated with 200 μM HNO for 10 and 20 min, respectively; In each group: ER-JN bioimage from red channel. DiOC₆(3) bioimage from green channel. Hoechst 33342 bioimage from blue channel. Overlay of red channel, green channel and blue channel, and overlay of red channel, green channel, blue channel and bright field. Red channel: $\lambda_{\text{ex}} = 690 \text{ nm}$, $\lambda_{\text{em}} = 700\text{--}800 \text{ nm}$; Green channel $\lambda_{\text{ex}} = 488 \text{ nm}$, $\lambda_{\text{em}} = 560\text{--}600 \text{ nm}$; Blue channel: $\lambda_{\text{ex}} = 405 \text{ nm}$, $\lambda_{\text{em}} = 420\text{--}480 \text{ nm}$

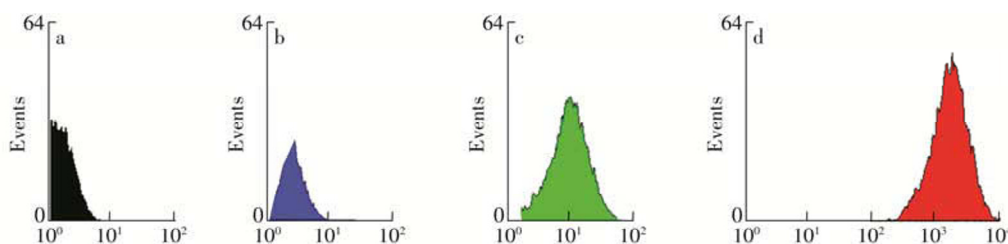


Fig.8 Representative data of flow-cytometric analysis

(a) Control; (b) The cells were incubated with 1 μM ER-JN for 15 min, then washed with DMEM three times to remove the overdose probe; (c) The cells were treated as described in (b), then incubated with 200 μM HNO for 10 min; (d) The cells were treated as described in (c), then exposed to another dosages of 200 μM HNO for an additional 10 min

3.6 Flow cytometric analysis

Laser scanning confocal microscope is suitable for analysis of a relatively small numbers of cells only in visual fields, while flow cytometry (FCM) can detect millions of cells sensitively and rapidly, and provide more statistically reliable results. Therefore, flow cytometric analysis was also employed to analyze the fluorescence changes in living cells caused by HNO. As shown in Fig.8, the X axis represents fluorescent intensity and the Y axis represents cells counts. The cells were divided into four groups: group **a** was a blank group set for control; in group **b**, the cells were incubated with ER-JN for 15 min and then washed with DMEM; in group **c**, the cells were treated as described in group **b**, and then incubated with 200 μM HNO for another 10 min; in group **d**, the cells were treated as described in group **c**, and then exposed to another 200 μM for 10 min. It was obvious that cells in group **a** and **b** had faint fluorescence, and the cells in group **c** with the addition of HNO emitted relatively stronger fluorescence, whereas more significant increase of fluorescence in group **d** with the addition of double dosage of HNO was obtained. The FCM results were in consistent with the fluorescence imaging results shown in Fig.7, indicating that the synthesized probe ER-JN could be used to detect the changes of HNO concentration in living cells qualitatively and quantitatively.

4 Conclusions

In summary, a novel NIR fluorescent probe ER-JN was synthesized in this work, with aza-BODIPY as fluorophore and triphenylphosphine as recognition unit, for detection of changes of HNO concentration in living cells. The ER-JN probe exhibited remarkable “turn-on” fluorescence response towards HNO and showed high selectivity, good sensitivity and low cytotoxicity. Moreover, the probe could locate in endoplasmic reticulum and be used to detect the changes of HNO concentrations in living cells. These results demonstrated that probe ER-JN had great significance and practical value for the research of biological and pathological

functions of HNO in subcellular fractions, living cells, organs and even in living organism.

References

- [1] Irvine J C, Ritchie R H, Favaloro J L, Andrews K L, Widdop R E, Kemp-Harper B K. *Trends Pharmacol. Sci.*, **2008**, 29(12): 601–608
- [2] Paolucci N, Jackson M I, Lopez B E, Miranda K, Tocchetti C G, Wink D A, Hobbs A J, Fukuto J M. *Pharmacol. Ther.*, **2007**, 113(2): 442–458
- [3] Favaloro J L, Kemp-Harper B K. *Cardiovasc. Res.*, **2007**, 73(3): 587–596
- [4] Paolucci N, Saavedra W F, Miranda K M, Martignani C, Isoda T, Hare J M, Espey M G, Fukuto J M, Feelisch M, and Wink D A. *Proc. Natl. Acad. Sci. USA.*, **2001**, 98(18): 10463–10468
- [5] Dutton A S, Fukuto J M, Houk K. *J. Am. Chem. Soc.*, **2004**, 126(12): 3795–3800
- [6] Malinski T, Taha Z, *Nature*, **1992**, 358(6388): 676–678
- [7] Nagano T, Yoshimura T. *Chem. Rev.*, **2002**, 102(4): 1235–1270
- [8] Li X, Gao X, Shi W, Ma H. *Chem. Rev.*, **2014**, 114(1): 590–596
- [9] Wang R, Yu C, Yu F, Chen L. *TrAC. Trends Anal. Chem.*, **2010**, 29: 1004–1013
- [10] Wrobel A T, Johnstone T C, Deliz Liang A, Lippard S J, Rivera-Fuentes P. *J. Am. Chem. Soc.*, **2014**, 136(12): 4697–4705
- [11] McQuade L E, Lippard S J. *Curr. Opin. Chem. Biol.*, **2010**, 14(1): 43–49
- [12] Zhou Y, Liu K, Li J, Fang Y, Zhao T, Yao C. *Org. Lett.*, **2011**, 13(6): 1290–1293
- [13] Wang R, Yu F, Chen L, Chen H, Wang L, Zhang W. *Chem. Commun.*, **2012**, 48(96): 11757–11759
- [14] Wang R, Yu F, Liu P, Chen L. *Chem. Commun.*, **2012**, 48(43): 5310–5312
- [15] Jing X, Yu F, Chen L. *Process in Chemistry*, **2014**, 26(5), 866–878
- [16] Gao M, Yu F, Chen L. *Process in Chemistry*, **2014**, 26(6),

- 1065–1078
- [17] Wang R, Chen L, Liu P, Zhang Q, Wang Y Q. *Chem. Eur. J.*, **2012**, 18(36): 11343–11349
- [18] Gao M, Yu F, Chen H, Chen L. *Anal. Chem.*, **2015**, 87(7): 3631–3638
- [19] Gao M, Wang R, Yu F, You J, Chen L. *Analyst*, **2015**, 140(11): 3766–3772
- [20] Jing X, Yu F, Chen L. *Chem. Commun.*, **2014**, 50: 14253
- [21] Liu P, Jing X, Yu F, Lv C, Chen L. *Analyst*, **2015**, 140(13), 4576–4583